

Sedimentary Mercury Enrichments as a Tracer of Large Igneous Province Volcanism

Lawrence M. E. Percival¹, Bridget A. Bergquist², Tamsin A. Mather³, and Hamed Sanei⁴

ABSTRACT

Volcanic activity associated with the emplacement of Large Igneous Provinces (LIPs) has been linked to most Phanerozoic extinctions/episodes of major environmental change. In recent years, mercury (Hg) enrichments and elevated mercury/total organic carbon (Hg/TOC) ratios have been increasingly utilized as a marker of volcanism in sedimentary records deposited distally from LIPs. The proxy is based on the premise that volcanism is a major natural source of the element to the atmosphere, and was especially important prior to anthropogenic emissions. To date, end-Permian and end-Triassic records illustrate the strongest use of Hg as a volcanic proxy; aided by supporting evidence (including Hg isotopes) for LIP eruptions and/or volatile emissions. Sedimentary records of several other events also document Hg enrichments in at least one region, suggesting regional or global Hg-cycle perturbations potentially linked to volcanism at those times. The Cenomanian-Turonian Oceanic Anoxic Event appears to be an exception, with Hg/TOC peaks documented in a small minority of studied records, suggesting minimal Hg-cycle disturbance at that time. Even for events that apparently featured a global-scale Hg-cycle perturbation, variable Hg enrichments across individual archives of that same crisis indicate that the complex biogeochemical cycling of the element can strongly influence local/regional aquatic, biological, or sedimentary processes to alter the precise signature of any worldwide disturbance. Recent studies are beginning to investigate these complexities, but further work is needed to fully explore the nuances of Hg in the geological record, and how it can be best employed as a proxy for LIP volcanism.

11.1. INTRODUCTION

Volcanic activity related to the emplacement of Large Igneous Provinces (LIPs) has long been thought to play a significant causal role in several episodes of environmental perturbation during the Phanerozoic Eon, often resulting in major mass extinctions (e.g., Rampino & Strothers, 1988; Wignall, 2001, 2005; Courtillot & Renne, 2003;

Bond & Wignall, 2014; Bond & Sun, Chapter 3 this volume). This hypothesis of volcanically stimulated climatic/biospheric stress is based chiefly on a very strong correlation between the established dates of Phanerozoic events of environmental/biospheric change and the radioisotopically determined ages of igneous rocks associated with various LIPs (Fig. 11.1; see also recent studies by Svensen et al., 2012; Blackburn et al., 2013; Sell et al., 2014; Burgess & Bowring, 2015; Renne et al., 2015; Schoene et al., 2015; Davies et al., 2017; and the review of Kasbohm et al., Chapter 2 this volume). However, correlating the ages of LIP volcanics and extinction/climate episodes in this way is hindered by uncertainties attendant in the determination and comparison of stratigraphic age models and radioisotopic dates, and a lack of precise ages for several geologic events and LIP eruptions. Moreover, the volcanic

¹Analytical, Environmental and Geochemistry Research Group, Vrije Universiteit Brussel, Brussels, Belgium

²Department of Earth Sciences, University of Toronto, Toronto, Ontario, Canada

³Department of Earth Sciences, University of Oxford, Oxford, United Kingdom

⁴Department of Geoscience, Aarhus University, Aarhus, Denmark

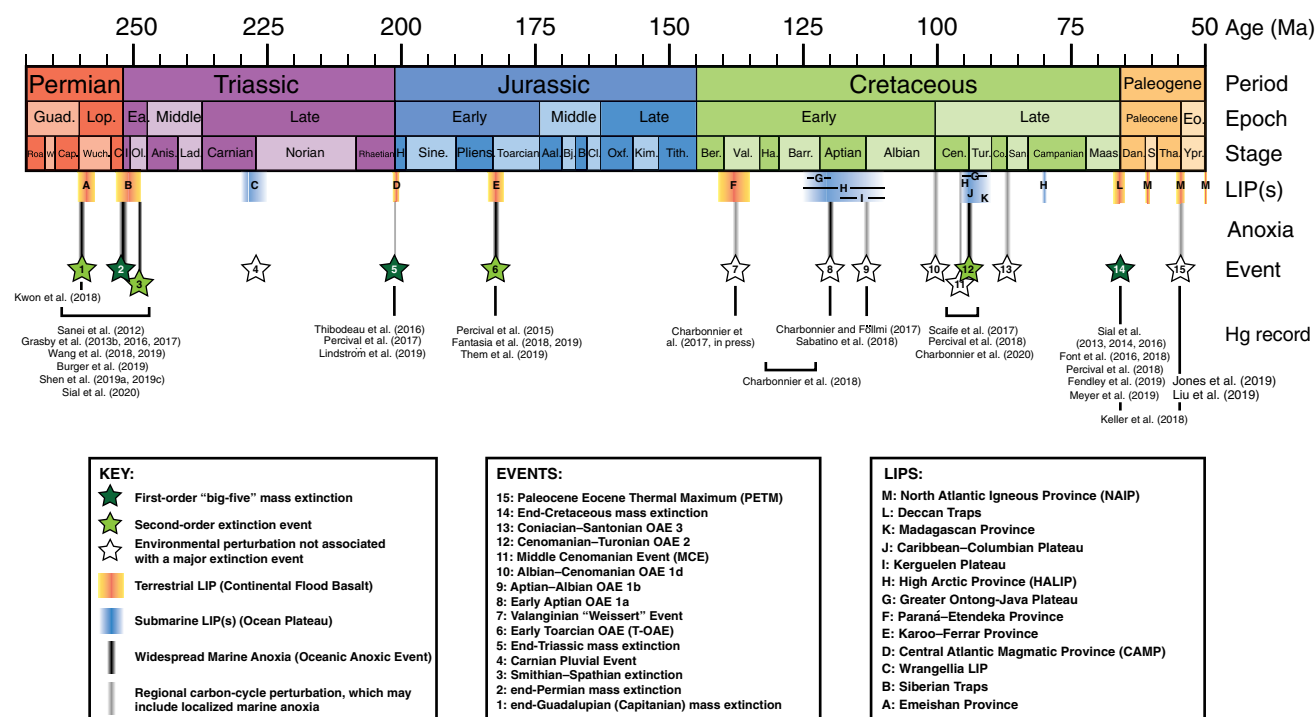


Figure 11.1 LIPs, mass extinctions, and environmental perturbations. Illustration of the temporal correlation between extinction events, major environmental perturbations, carbon-cycle perturbations, and LIP emplacement from the Late Permian to the Paleogene, based on Percival et al. (2018). Events for which Hg studies have been undertaken are indicated. Note that Hg studies have also been published for the Cambrian (Faggetter et al., 2019; Pruss et al., 2019), Ordovician-Silurian (444 Ma, Gong et al., 2017; Jones et al., 2017; Shen et al., 2019b; Smolarek-Lach et al., 2019), Frasnian-Famennian (372 Ma, Racki et al., 2018a), and Devonian-Carboniferous (359 Ma, Racki et al., 2018b; Kavolda et al., 2019, Paschall et al., 2019) extinctions, which do not appear within this timescale.

activity of many LIPs began prior to or continued after the environmental/biospheric crises with which they are associated. This last point relates to the proposed causal mechanisms linking LIP volcanism to climate/extinction events revolving around the release of volcanogenic volatiles (e.g., CO_2 and SO_2) to the atmosphere, rather than the emplacement/eruption of igneous material (see Mather & Schmidt, Chapter 4 this volume). Therefore, while it is expected that the onset and duration of any environmental change (and/or any resulting extinctions) would have coincided with the times of high volatile output associated with LIP emplacement, such emissions will not necessarily be directly proportional to erupted/intruded volumes of magma, and both parameters may vary considerably over the lifetime of a LIP (Schoene et al. 2019; Sprain et al., 2019; Eddy et al., 2020). Additionally, it has been proposed that the most environmentally damaging gas emissions associated with LIPs were not necessarily magmatic in origin, but instead might have resulted from the metamorphism of volatile-rich sediments by the emplacement of intrusive sills (e.g., Svensen et al., 2004, 2009; McElwain et al., 2005; Ganino & Arndt, 2009; Burgess & Bowring, 2015; Davies et al., 2017).

Recently, sedimentary mercury (Hg) enrichments (as characterized by elevated Hg concentrations and Hg/total organic carbon ratios) have been proposed as a potential proxy for volcanic activity and volatile release (Sanei et al., 2012). A major natural source of Hg to the atmosphere is emission of the element as a trace volcanic gas, which has the potential for global distribution through the atmosphere (see below and Fig. 11.2a). Consequently, increased Hg concentrations in sedimentary strata that record episodes of mass extinction/environmental perturbation are frequently interpreted as evidence for large-scale volcanism and/or volatile release at those times, which may have acted as the trigger for the biospheric/climatic crisis. Such peaks in Hg content have been reported from records of all five major Phanerozoic extinctions, as well as various other climatic perturbations such as the Oceanic Anoxic Events (OAEs) and the Paleocene-Eocene Thermal Maximum (e.g., Sanei et al., 2012; Percival et al., 2015; Font et al., 2016; Thibodeau et al., 2016; Charbonnier & Föllmi, 2017; Charbonnier et al., 2017; Jones et al., 2017; Scaife et al., 2017; Keller et al., 2018; Racki et al., 2018a). Here, the published records of these Hg enrichments are reviewed,

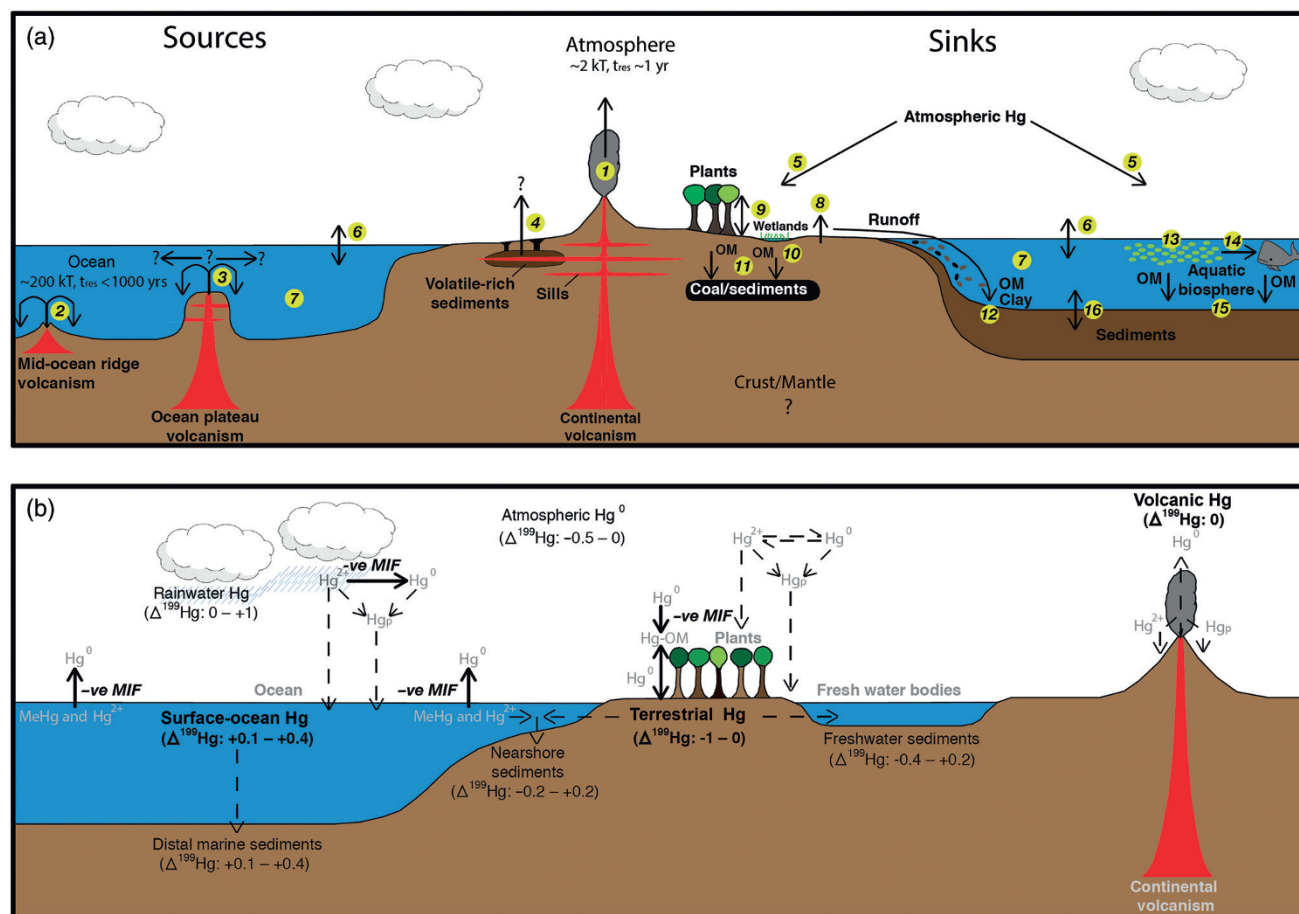


Figure 11.2 (a) The natural mercury cycle, a simplified illustration from Percival et al. (2018). Atmospheric and oceanic residence times of Hg are indicated (Slemr et al., 1985; Gill and Fitzgerald, 1988; Blum et al., 2014; Gustin et al., 2015). Processes affecting the source, sink, and transportation of mercury through the ocean-atmosphere system are indicated as follows: (1) Volcanic emission of mercury, chiefly as gaseous elemental mercury (Hg⁰) to the atmosphere; (2) Hydrothermal emission of Hg to the ocean at midocean ridges; (3) Presumed release of hydrothermal Hg to the ocean from submarine ocean plateau volcanism, similar to that at midocean ridges; (4) Possible emission of thermogenic Hg to the atmosphere following heating of organic-rich sediments by intruding sills; (5) Removal of atmospheric Hg to land, water, or forest canopy, either as direct uptake of gaseous Hg⁰ by plants or deposition of particulate Hg (dry deposition) and soluble oxidized mercury (Hg²⁺) following interactions between atmospheric Hg⁰ and atmospheric oxidizing agents such as halogen, nitrile, ozone, and hydroxyl radicals (wet deposition); (6) Air-water interchange of Hg⁰; (7) Conversion of mercury species between Hg⁰, Hg²⁺, and MeHg (monomethylmercury and dimethylmercury) through multiple biotic and abiotic reactions in aquatic environments (for example, Fitzgerald et al., 2007; Selin, 2009; Blum et al., 2014; Bowman et al., 2015); (8) Reduction of soil Hg to Hg⁰, which is subsequently reemitted to the atmosphere; (9) Interchange of mercury between soil and forest canopy through emission of soil Hg and decay of leaves that have taken up Hg; (10) High abundance of sulfate- and/or iron-reducing bacteria in reduced wetland environments promoting methylation of Hg²⁺ to organophilic monomethylmercury (MMHg), which can adsorb onto organic matter; (11) Deposition of sediments in soil Hg-OM complexes to peats or coals; (12) Riverine runoff (and potentially deposition) into lacustrine or marine environments of detrital Hg bound to either organic matter or clay minerals; (13) Uptake of Hg²⁺ or MMHg by aquatic biota; (14) Bioaccumulation of organophilic MMHg up the food chain; (15) Deposition of Hg into sediments as Hg-OM complexes; (16) Potential remobilization and release of sedimentary Hg into the aquatic realm. (b) Mass independent fractionation (MIF) of mercury in a simplified illustration of the mercury cycle. Grey lettering indicates a source or inventory of Hg at the Earth's surface, and changes in the speciation of mercury (Hg⁰ = inert gaseous elemental mercury; Hg²⁺ = reactive oxidized mercury; MeHg = mono- or di-methylmercury; Hg-OM = organo-mercury complexes). Black lettering indicates inventories of Hg and their average $\Delta^{199}\text{Hg}$ composition in the modern (values taken from data in the model of Sonke, 2011; and the review of Blum et al., 2014), and pathways of Hg where MIF may occur. Bold arrows also indicate pathways of Hg where MIF occurs (e.g., photochemical reduction in surface-marine waters or raindrops, and uptake of Hg by plants/lichens). Thinner dashed arrows indicate pathways of Hg where MIF is not known to occur.

and the possible conclusions regarding how mercury operated during times of extinction/environmental perturbation and the use of this element as a proxy for volcanism are discussed.

11.1.1. The Natural Mercury Cycle

Volcanic outgassing represents a major natural (nonanthropogenic) source of mercury to the Earth's surface in the modern (e.g., Schroeder & Munthe, 1998; Pyle & Mather, 2003; Bagnato et al., 2007, 2011, 2014). Volcanic Hg is largely emitted to the atmosphere as a gaseous elemental species (Hg^0), with a smaller fraction erupted as oxidized or particulate species that have shorter atmospheric lifetimes and are likely to be deposited locally (Bagnato et al., 2007). Hg^0 has a typical atmospheric residence time on the order of about 1 year. Removal of the element from the atmosphere typically occurs via oxidation by various species (e.g., halogen radicals, nitrous oxide, ozone) to Hg^{2+} , followed by either “dry” or “wet” deposition to the terrestrial and aquatic realms (see Fig. 11.2a; Schroeder & Munthe, 1998; Selin, 2009). Additionally, Hg^0 in the atmosphere can be directly taken up by plant foliage (e.g., Ericksen et al., 2003; Demers, 2013; Enrico et al., 2016), and transferred into soils via leaf-litter deposition (Obrist, 2007; Wang et al., 2016). A small fraction of gaseous Hg^0 may also be directly adsorbed into soils (Obrist et al., 2011). The majority of soil Hg is thought to be buried bound to organic compounds, but a small fraction may be reduced and returned to the atmosphere as Hg^0 (e.g., Lindberg et al., 1998; Obrist, 2007; Wang et al., 2016; Obrist et al., 2018). In the aquatic realm, a range of biotic and abiotic reactions can transform mercury between elemental Hg^0 (which may then be reemitted to the atmosphere), oxidized Hg^{2+} , or toxic monomethyl-/dimethylmercury (see review by Fitzgerald et al., 2007). The methylation of mercury typically occurs in poorly oxygenated aquatic settings (e.g., bottom waters and sediment pore waters) and is largely facilitated by microbes (e.g., Fitzgerald & Lamborg, 2014). Ultimately, aquatic mercury is either evaded to the atmosphere as Hg^0 or deposited to sediments, typically bound to organic compounds. Consequently, concentrations of the element tend to correlate well with the total organic carbon (TOC) content in modern sediments (e.g., Sanei & Goodarzi, 2006; Outridge et al., 2007; Liu et al., 2012; Ruiz & Tomiyasu, 2015), resulting in a Hg/TOC ratio that should remain relatively constant under stable conditions in a particular setting. Thus, studies of sedimentary mercury normalize the Hg concentration to the TOC content (see Sanei et al., 2012). An increased Hg content in waters with no change in TOC will lead to higher Hg/TOC ratios that might indicate an increased external influx of Hg to that environment (see, e.g., Jin & Liebezeit, 2013; Sanei et al., 2014; Daga

et al., 2016). Sulfides and clay minerals can also scavenge mercury from the water column, and in certain environments deposition of mercury with those species might override the usual sedimentary Hg-organic matter relationship (see Sanei et al., 2012; Charbonnier & Föllmi, 2017; and Percival et al., 2018). However, more work is needed to determine in what sedimentary contexts it is most prudent to normalize Hg against which species, and normalizing against all of them may be of use for some records (see Grasby et al., 2019). Southern Ocean diatomite sediments of Holocene age have also been noted as featuring large Hg concentrations, suggesting that biogenic silica might also be a potentially important sink of oceanic Hg in this context (Zaferani et al., 2018), although it is currently unknown whether this relationship also applies in other oceanographic settings or if biogenic silica would preserve changes to the global Hg cycle in the deep-time geological record. Submarine volcanism also emits Hg to the aquatic realm (e.g., Lamborg et al., 2006; Bagnato et al., 2014); however, the influence of subaqueous volcanic Hg emissions appears to be limited to only the regional marine environment immediately proximal to that volcanic system (Bowman et al., 2015). Consequently, it is not clear to what extent submarine volcanism can perturb the global Hg cycle.

11.1.2. Mercury Isotopes

In addition to sedimentary Hg concentrations and Hg/TOC ratios, variations in the natural stable isotopes of Hg are also being applied to understanding past Hg perturbations in the geological record. Mercury has seven stable isotopes: ^{196}Hg (0.16%), ^{198}Hg (10.04%), ^{199}Hg (16.94%), ^{200}Hg (23.14%), ^{201}Hg (13.17%), ^{202}Hg (29.73%), and ^{204}Hg (6.83%), which can undergo both mass-dependent (MDF) and mass-independent (MIF) fractionation in the natural environment. MDF, reported as variations in the $^{202}\text{Hg}/^{198}\text{Hg}$ ratio in delta notation ($\delta^{202}\text{Hg}$), occurs during many transformations including redox, biological, and phase changes. In contrast, large MIF for Hg only occurs during photochemical reactions with odd isotopes displaying MIF during aqueous photochemical reactions (reported as $\Delta^{199}\text{Hg}$), and even MIF occurring during gas phase atmospheric photochemical reactions (reported as $\Delta^{200}\text{Hg}$) (see Blum et al., 2014). This review focuses on the application of sedimentary mercury isotope compositions to understanding past volcanic events, focusing on odd-isotope MIF ($\Delta^{199}\text{Hg}$); a more comprehensive review of mercury-isotope systematics in natural processes is given by Blum et al. (2014). Constraints on the isotopic composition of mercury emissions from modern volcanism are limited to only one study (Zambardi et al., 2009), which reported mercury with a $\delta^{202}\text{Hg}$ composition between 0 ‰ and -2 ‰, and no measureable MIF (i.e.,

$\Delta^{199}\text{Hg} = 0\text{‰}$). This work represented only one volcanic system and focused on an arc-setting not analogous with LIPs, for which the isotopic signature of volcanically emitted Hg^0 might have been rather different. However, the results are consistent with other investigations of geogenic Hg-isotope compositions (in settings where the Hg has not undergone any atmospheric or aqueous cycling) that also reported similar $\delta^{202}\text{Hg}$ compositions and a lack of MIF (see Blum et al., 2014). It should be noted though that MDF can be caused by biological, physical, and chemical processes at the Earth's surface, and potentially post-depositionally (see Blum et al., 2014; Thibodeau et al., 2016). Thus, several studies recommend caution in interpreting sedimentary $\delta^{202}\text{Hg}$ values between 0 ‰ and -2 ‰ as evidence of volcanic influx, as they may not be representative of the original source composition (e.g., Thibodeau et al., 2016; Grasby et al., 2017; Thibodeau & Bergquist, 2017). Nonetheless, trends in MDF may still reflect important changes in the Hg cycle and sources to it (Grasby et al., 2017), and may become more useful in the future with more understanding of Hg MDF preservation in sediments.

Consequently, trends in MIF of mercury (specifically $\Delta^{199}\text{Hg}$) are currently more helpful for investigating records of environmental change potentially driven by volcanism, as volcanic (and nonphotochemically cycled) Hg likely has an isotopic signature distinct from inventories of that element that has undergone significant cycling through surface reservoirs. Mostly, odd-isotope MIF of mercury is thought to be dominated by two main processes at the Earth's surface. First, the photochemical reduction of aqueous Hg^{2+} to Hg^0 in surface waters and raindrops (Bergquist & Blum, 2007; Demers et al., 2013), which produces negative $\Delta^{199}\text{Hg}$ values in the resultant Hg^0 gas (and consequently a slightly negative $\Delta^{199}\text{Hg}$ composition in the atmospheric inventory) and a residual pool of aqueous Hg^{2+} with a more positive $\Delta^{199}\text{Hg}$ signature (Fig. 11.2b). Second, during the uptake of Hg^0 by foliage (e.g., Carignan et al., 2009; Demers et al., 2013), there is additional MIF that enriches the plant matter in Hg with a $\Delta^{199}\text{Hg}$ composition even more negative than that of atmospheric mercury (Fig. 11.2b). Consequently, soils typically have negative $\Delta^{199}\text{Hg}$ compositions because the pathway of Hg to them is dominated by leaf litter fall (e.g., Demers et al., 2013). In general, marine sediments receive Hg from two main sources: (1) incorporation of aqueous Hg^{2+} deposition with positive $\Delta^{199}\text{Hg}$ and (2) runoff from terrestrial soils with negative $\Delta^{199}\text{Hg}$ (Blum et al., 2014). Thus, Hg in sediments typically features either significant positive or negative MIF, depending on the relative proportion of the two major pathways of Hg entering the ocean or body of water (Thibodeau & Bergquist, 2017). Positive sedimentary $\Delta^{199}\text{Hg}$ values

reflect a predominantly atmospheric Hg influx most commonly observed in strata that were deposited in a marine environment far from land. In contrast, nearshore-marine and terrestrial sediments where Hg deposition is dominated by runoff from land tend to have negative $\Delta^{199}\text{Hg}$ compositions, consistent with an influx of Hg from soils. Because volcanic Hg is thought to be devoid of MIF at the point of emission, it has been proposed that a sedimentary Hg enrichment that lacks a MIF signature could reflect an increased output of Hg by volcanoes, which has either overwhelmed or bypassed the MIF inducing processes detailed above (e.g., Thibodeau et al., 2016). However, it should be noted that considerable work is still needed to fully understand all processes that can result in isotopic variations in Hg reservoirs (Blum et al., 2014). For example, it has recently been proposed that negative MIF could also arise in sediments deposited under strongly euxinic marine conditions (Zheng et al., 2018).

11.2. DISCUSSION OF GEOLOGICAL MERCURY RECORDS

11.2.1. Do Stratigraphic Records of All Major Events Document Hg-Cycle Perturbations?

Of key significance in interpreting geological records of the past Hg cycle is the necessity to investigate multiple stratigraphic archives from different locations. The importance of adopting this multisite approach is demonstrated by the mercury records of the Cenomanian-Turonian OAE 2 (94 Ma). Increased Hg concentrations and Hg/TOC ratios were initially reported from OAE 2 strata in the southern part of the Western Interior Seaway (Texas, USA) and Demerara Rise in the central Atlantic, from which a Hg-cycle perturbation was inferred (Scaife et al., 2017; Percival et al., 2018). However, further studies of boreal, Tethyan, and Indian Ocean records have shown that the majority of OAE 2 records do not feature clear evidence of increased Hg contents or Hg/TOC ratios; thus, it appears that any Hg-cycle perturbation during OAE 2 was at most only regional in extent (Percival et al., 2018). Similarly, sedimentary strata recording the Smithian-Spathian extinction (250 Ma) feature elevated Hg/TOC in the Arctic (Grasby et al., 2013b, 2016; Hammer et al., 2019) but more variable trends across South China, Indian Tethyan, and Panthalassic records (Wang et al., 2019; Shen et al., 2019a). Therefore, it should not be assumed that Hg enrichments observed from one area are manifestly indicative of a global Hg-cycle perturbation.

At present, widespread records of Hg enrichments spanning multiple continents exist for only a few events. The end-Ordovician extinction (444 Ma), end-Permian

extinction (252 Ma), end-Triassic extinction (201 Ma), Toarcian OAE (183 Ma), and end-Cretaceous extinction (66 Ma), all feature Hg enrichments that can be correlated on the basis of biostratigraphic or carbon-isotope information across numerous sedimentary sequences spanning multiple regions/continents and both hemispheres (Sanei et al., 2012; Grasby et al., 2013b, 2016, 2017; Sial et al., 2013, 2014, 2016, 2020; Percival et al., 2015, 2017, 2018; Font et al., 2016; Thibodeau et al., 2016; Gong et al., 2017; Jones et al., 2017; Fantasia et al., 2018, 2019; Keller et al., 2018; Wang et al., 2018; Burger et al., 2019; Fendley et al., 2019; Lindström et al., 2019; Meyer et al., 2019; Shen et al., 2019b, 2019c; Smolarek-Lach et al., 2019; Them et al., 2019). There are also widespread stratigraphic records of the Frasnian-Famennian (372 Ma), Devonian-Carboniferous (359 Ma), and Capitanian (end-Guadalupian, 260 Ma) extinctions, the Valanginian “Weissert” Event (135 Ma), and Paleocene-Eocene Thermal Maximum (PETM, 54 Ma) that feature Hg enrichments (Grasby et al., 2016; Charbonnier et al., 2017, in press; Keller et al., 2018; Kwon et al., 2018; Racki et al., 2018a, 2018b; Jones et al., 2019; Kalvoda et al., 2019; Liu et al., 2019; Paschall et al., 2019). However, it should be noted that the Toarcian, end-Cretaceous, and PETM Hg records show significant variation across the studied sites, indicating that local sedimentary and/or environmental factors strongly influenced Hg deposition in some locales at those times, in addition to any postulated global perturbation by volcanism (Percival et al., 2015, 2018; Jones et al., 2019). There is also no unambiguous candidate LIP for the end-Ordovician extinction currently, and it has been proposed that Hg enrichments in uppermost Ordovician-lowermost Silurian strata are redox controlled rather than volcanically sourced (Shen et al., 2019b).

Mercury enrichments have been also noted from Tethyan records of the early Aptian OAE 1a (121 Ma), and Aptian-Albian OAE 1b (113 Ma), as well as in a number of other Tethyan black shale horizons of Hauterivian-Barremian (Early Cretaceous, 133–125 Ma) age (Charbonnier & Föllmi, 2017; Charbonnier et al., 2018; Sabatino et al., 2018). However, because these Hg-cycle perturbations are all observed in Tethyan records, they do not give a global overview of the Hg cycle at those times. Similarly, although stratigraphic archives of two Cambrian events show Hg enrichments (Faggetter et al., 2019; Pruss et al. 2019), those records are currently restricted to single areas and might only document a regional Hg influx and/or local-process controls on mercury deposition.

It is less clear to what extent smaller non-LIP eruptions (e.g., arc volcanism) can perturb the local or global mercury cycle, with the quantities of Hg gas emitted during these more minor events assumed to be lower. Marine sediments studied for the Toarcian and Cenomanian

OAEs that were deposited proximally to arc systems did not show any Hg enrichments except within the event strata, suggesting that any local eruptions either did not perturb the local mercury cycle, or that any enrichments were not preserved in the geological record (Percival et al., 2015; Scaife et al., 2017; Fantasia et al., 2018). However, Racki et al. (2018a) did indicate possible correlations between Hg enrichments in marine sedimentary rocks and large arc eruptions. Local eruptions might be more easily preserved in the terrestrial realm. Andean eruptions (together with local wildfires) have been proposed as resulting in Hg enrichments of modern-day wetland and lake sediments (e.g., Ribeiro Guevara et al., 2010; Daga et al., 2016). Percival et al. (2018) speculated that high Hg values in uppermost Cretaceous strata from Montana might be related to local arc volcanism (which is also evidenced by abundant tuff beds), although Fendley et al. (2019) concluded that local volcanism was unlikely to have been the cause of these peaks, and the Deccan Traps were also volcanically active when those sediments were deposited so a LIP source for the mercury could not be excluded.

11.2.2. Nonvolcanic Influences on Sedimentary Hg/TOC Variations

In addition to the widespread documentation of Hg-cycle perturbations, a further step in demonstrating that mercury enrichments can act as a tracer for volcanic activity is the confirmation that peaks in Hg/TOC ratios do not appear in sediments deposited at times when large-scale volcanism was not occurring. Figure 11.3 shows two such records studied by Grasby et al. (2013b) and Percival et al. (2015). The Kimmeridge Clay core records more than 1 Myr of Late Jurassic time, not thought to coincide with LIP emplacement. Very low Hg/TOC ratios, featuring minimal variations, are consistent with a lack of large-scale Hg emissions to the atmosphere at that time (Percival et al., 2015). Smith's Creek records elevations in Hg/TOC at the termination of the end-Permian extinction event and the Smithian-Spathian boundary, both of which are thought to coincide with pulses of Siberian Trap volcanism (Grasby et al., 2013b). However, the remainder of the sequence, which documents some 5 Myr of Early Triassic time, features relatively low and constant Hg/TOC values. Both archives document local redox changes evidenced by variability in TOC, pyrite abundance, and/or trace metal content (Morgans-Bell et al., 2001; Grasby et al., 2013a), but neither shows a correlation between those redox changes and Hg/TOC ratios, suggesting that localized variations in marine oxygenation do not necessarily influence Hg deposition. In contrast, other studies (of Late Cambrian and Ordovician-Silurian boundary records) have concluded that local changes in redox

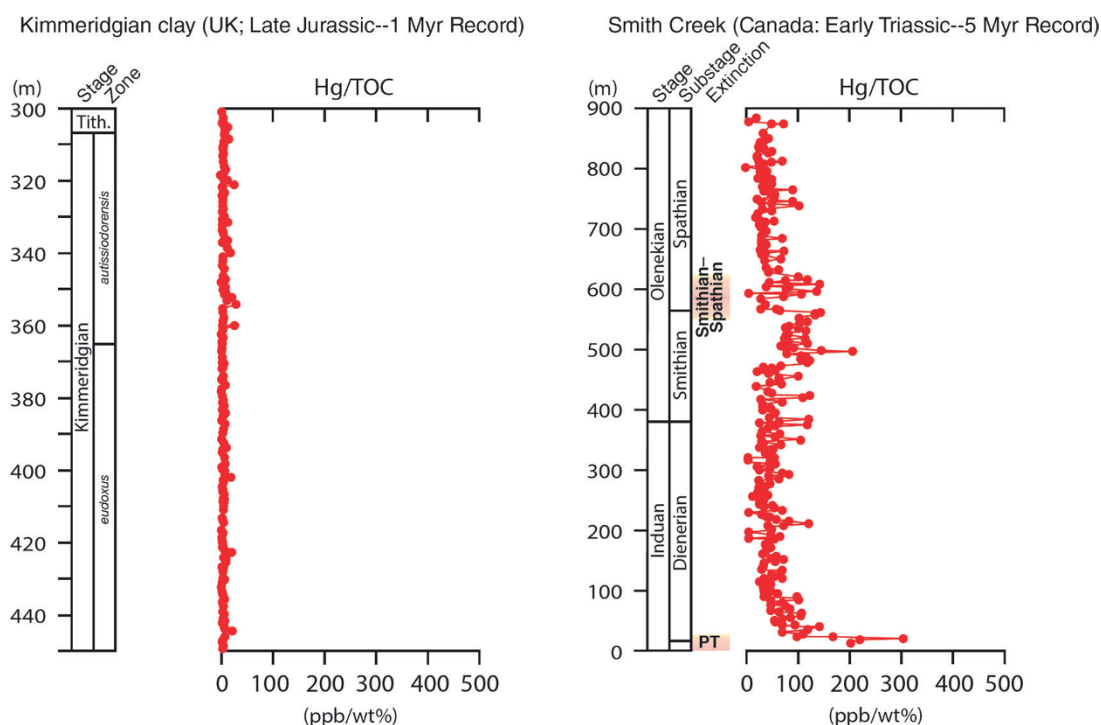


Figure 11.3 Hg trends during nonvolcanic times. Published Hg/TOC trends from the Early Triassic and Late Jurassic long-term records of Smith Creek (Canada) and the Kimmeridge clay (England, UK), respectively. Temporal information and Hg/TOC data for the Kimmeridge clay (including ammonite zones) is from Percival et al. (2015) and for Smith Creek from Grasby et al. (2013b). The positioning of times of LIP volcanism associated with the end-Permian (PT) and Smithian-Spathian intervals at Smith Creek is postulated based on Grasby et al. (2013b).

could indeed have influenced mercury deposition, based on a correlation of Hg and Hg/TOC with glauconite and pyrite content (Shen et al., 2019b; Pruss et al., 2019). However, it should be noted that no oceanic crust is preserved from the time of interest for either study, so a LIP source cannot be totally excluded in either case. Also, pyrite sequestration has been proposed as playing an important role in the draw-down of Hg from LIP volcanism in some settings, especially where organic-matter burial is limited (Sanei et al., 2012).

However, lithological variations arising from redox changes certainly can impact Hg/TOC ratios. The Toarcian and Aptian OAEs in particular demonstrate this issue. In 10 out of 13 Toarcian OAE archives studied for mercury, Hg content increases (Percival et al., 2015; Fantasia et al., 2018; Them et al., 2019). However, 4 of those records also document marked elevations in TOC, potentially overprinting any volcanic signal at those locations (see Percival et al., 2015). A similar phenomenon has been proposed for Aptian OAE records, where high TOC contents are thought to mute the magnitude of observed Hg/TOC peaks (Charbonnier & Föllmi, 2017). A younger Pleistocene record of Mediterranean sapropels might also illustrate this point, with Hg/TOC ratios

noticeably lower in more organic-rich sapropel strata compared with background sediments, despite constant MIF values indicating that there was no change in the source of Hg to the immediate area (Gehrke et al., 2009). In fact, mercury concentrations increase within the sapropels, but are likely overprinted by the greater increase in TOC content. Very low TOC contents can also hinder interpretation of Hg/TOC ratios, as the low TOC values result in a very high Hg/TOC ratio that might vary dramatically depending on tiny changes in the TOC content. At present, Grasby et al. (2016) recommend not employing the Hg/TOC ratio for TOC contents under 0.2 wt%, in order to avoid generation of false Hg/TOC peaks that are unrelated to any increased Hg content (see Grasby et al., 2019, for a more in-depth discussion). Future increases in the precision of TOC measurements may mean that this recommendation can be revised. There is little published information on how sediment heating/oxidation may affect Hg/TOC ratios, although one study of Cenomanian-Turonian OAE 2 records suggests that TOC loss during organic-matter maturation may exaggerate Hg/TOC values and generate “false” volcanic peaks, in which case preservation and/or type of organic matter should be scrutinized when interpreting Hg/TOC

trends (Charbonnier et al., 2020). Regardless, the key point in interpreting Hg/TOC trends is that elevated Hg/TOC ratios should not be interpreted as a volcanic signal unless they are correlative with an increase in the Hg concentration (i.e., there has been an increased influx/burial of Hg above and beyond the normal drawdown by organic material). Both increased Hg/TOC values derived from a fall in TOC content, and elevated Hg concentrations unaccompanied by a rise in Hg/TOC, cannot be unambiguously stated as being derived from an increase in the overall input of Hg (from volcanism or otherwise) because an alternative driver such as lithological changes could also have caused those variations (see also Grasby et al., 2019).

Finally, in addition to volcanic Hg emissions, there may be alternative sources of mercury that can perturb ocean-atmosphere reservoirs. Heating of organic-rich sedimentary rocks by intrusive sills may have supplemented magmatic Hg with thermogenic emissions of the element (see, e.g., Svensen et al., 2004; Percival et al., 2015; Jones et al., 2019), although such outgassing would likely still be related to LIP emplacement. Another possibility is a major release of Hg from soils and forests, since they are the largest surface reservoir of the element (Fitzgerald & Lamborg, 2014). A large runoff of terrigenous material during a time of enhanced continental weathering could cause a sedimentary enrichment in Hg, potentially also recycling any volcanically emitted Hg (Them et al., 2019; Hammer et al., 2019). Burning of coal/biomass via magmatic intrusions or wildfires may also release Hg as Hg⁰ gas or bound to coal fly ash or charcoal particles (e.g., Sanei et al., 2012; Grasby et al., 2017). Thermogenic, runoff, and wildfire processes are thought to have acted during a number of Phanerozoic environmental perturbations, and may act as supplementary, recycled, or alternative sources of Hg to sediments (Grasby et al., 2019). However, an influx of Hg to marine sediments from wildfire or terrigenous sources can be tested on the basis of whether a Hg enrichment correlates with other evidence such as charcoal/fly ash, Hg-isotopic excursions, or other markers of terrigenous material. Thus, attributing global enrichments in Hg to volcanism is strongest when also correlated with other possible markers of volcanism.

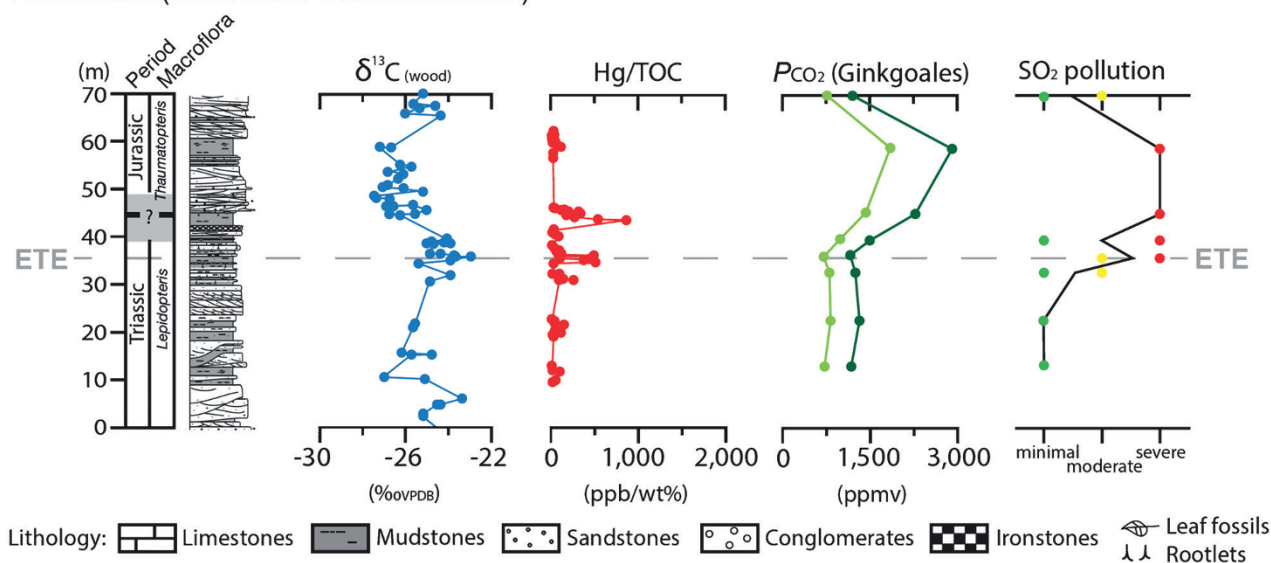
11.2.3. Correlating Hg enrichments with other evidence of LIP volcanism

For two events associated with LIP volcanism, the end-Triassic extinction and Toarcian OAE, atmospheric contents of other gases potentially derived from volcanism or metamorphism of volatile-rich country rocks by LIP magmas (e.g., carbon dioxide, CO₂; sulfur dioxide, SO₂) have been reconstructed on the basis of plant fossils from the same stratigraphic records investigated for mercury

(McElwain et al., 2005; Steinthorsdottir et al., 2011, 2018; Bacon et al., 2013). A close (though not perfect) correlation is observed between trends in CO₂, SO₂ (end-Triassic only), and Hg and Hg/TOC (Fig. 11.4). The existence of these correlations within single sedimentary records may strengthen the case for production of all three gases by volcanic and/or thermogenic emissions, and volcanogenically triggered Hg-cycle perturbations during those two events.

However, for records of some geological events, there is clear geochronological/geochemical evidence of volcanism from other markers that do not match sedimentary Hg enrichments (although they are not proxies of volcanic gases). As already discussed, it is unclear whether there was a global perturbation in the Hg cycle during OAE 2, but there is clear evidence of volcanic activity at that time from a globally observed shift in sedimentary osmium-isotope ratios to unradiogenic (mantle) values (Turgeon & Creaser, 2008; Du Vivier et al., 2014, 2015; also see Dickson et al., Chapter 10 this volume, for an overview of osmium-isotope stratigraphy associated with LIP volcanism). The unclear evidence for sedimentary Hg enrichments suggests that this volcanism did not greatly influence the Hg cycle, possibly because a large part of the LIP volcanism at that time was likely submarine and any Hg emissions may have been less efficiently dispersed, generating the major spatial variability in mercury records associated with that event (see Percival et al., 2018). Similarly, while peaks in Hg and Hg/TOC have been reported from numerous end-Cretaceous sequences, the LIP volcanism associated with Cretaceous-Paleogene times (the Deccan Traps in India) commenced ~300 kyr earlier (e.g., Renne et al., 2015; Schoene et al., 2015), and is well documented in the sedimentary record by osmium-isotope evidence for major weathering of mantle-derived basalts (Ravizza & Peucker-Ehrenbrink, 2003; Robinson et al., 2009). Currently, there is little evidence for a perturbed Hg cycle during those 300 kyr (see Percival et al., 2018), suggesting that perhaps the initial Deccan volcanism had less of an impact on the global Hg inventory up until just prior to the extinction. There is also geochronological evidence that the Permian Siberian Traps (Russia), Toarcian Karoo-Ferrar (South Africa and Antarctica), and Valanginian Paraná-Etendeka (Namibia and Brazil) LIPs were volcanically active at times outside of those marked by sedimentary Hg enrichments (see Percival et al., 2018; Xu et al., 2018). Consequently, it is possible that not all volcanism leads to major perturbations in the atmospheric and surface reservoirs of Hg, which may instead be related to the amount, emplacement, and type of volcanism. Factors such as submarine versus subaerial eruptions, explosive versus effusive events, and intrusion of Hg- (organic-) rich country lithologies by intrusive LIP magmas may be particularly important in determining

Astartekløft (Greenland: Triassic-Jurassic)



Bornholm (Denmark: Toarcian OAE)

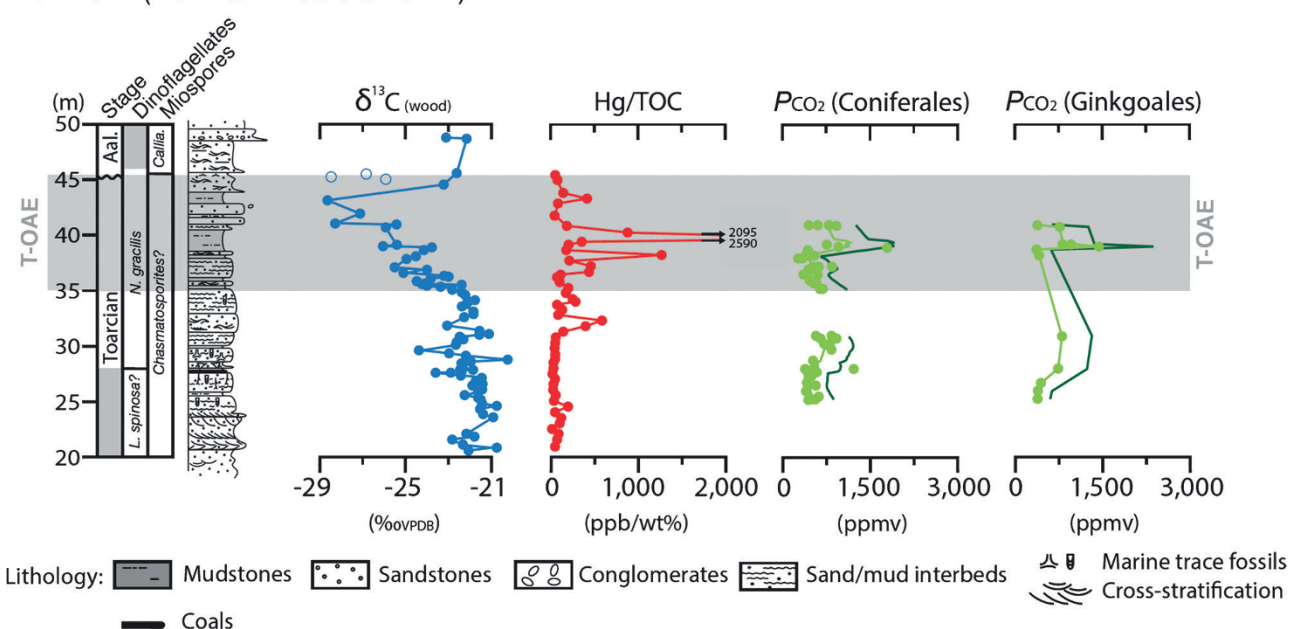


Figure 11.4 Evidence of atmospheric Hg versus other volcanogenic gases. Correlations between Hg/TOC records and reconstructed changes in atmospheric CO_2 and SO_2 based on plant fossil evidence for the Triassic-Jurassic record of Astartekløft (Greenland), and the Toarcian OAE (T-OAE) record of Bornholm (Denmark). For both the Triassic and Toarcian records, the Hg/TOC, CO_2 , and SO_2 (Triassic only) data are all from samples taken from these sections, permitting direct stratigraphic correlation. For Astartekløft, lithological and biostratigraphic information and carbon-isotope data are from Hesselbo et al. (2002); positioning of the end-Triassic extinction horizon (ETE) is based on Mander et al. (2013); Hg/TOC data are from Percival et al. (2017); CO_2 data are from Steinthorsdottir et al. (2011); SO_2 data are from Steinthorsdottir et al. (2018). For Bornholm, lithological and biostratigraphic information and carbon-isotope data are from Hesselbo et al. (2000); Hg/TOC data are from Percival et al. (2015); CO_2 data are from McElwain et al. (2005). For the CO_2 data at both locations, light green trends indicate modern standardization; dark green trends indicate Carboniferous standardization (see McElwain et al., 2005; and Steinthorsdottir et al., 2011, for details).

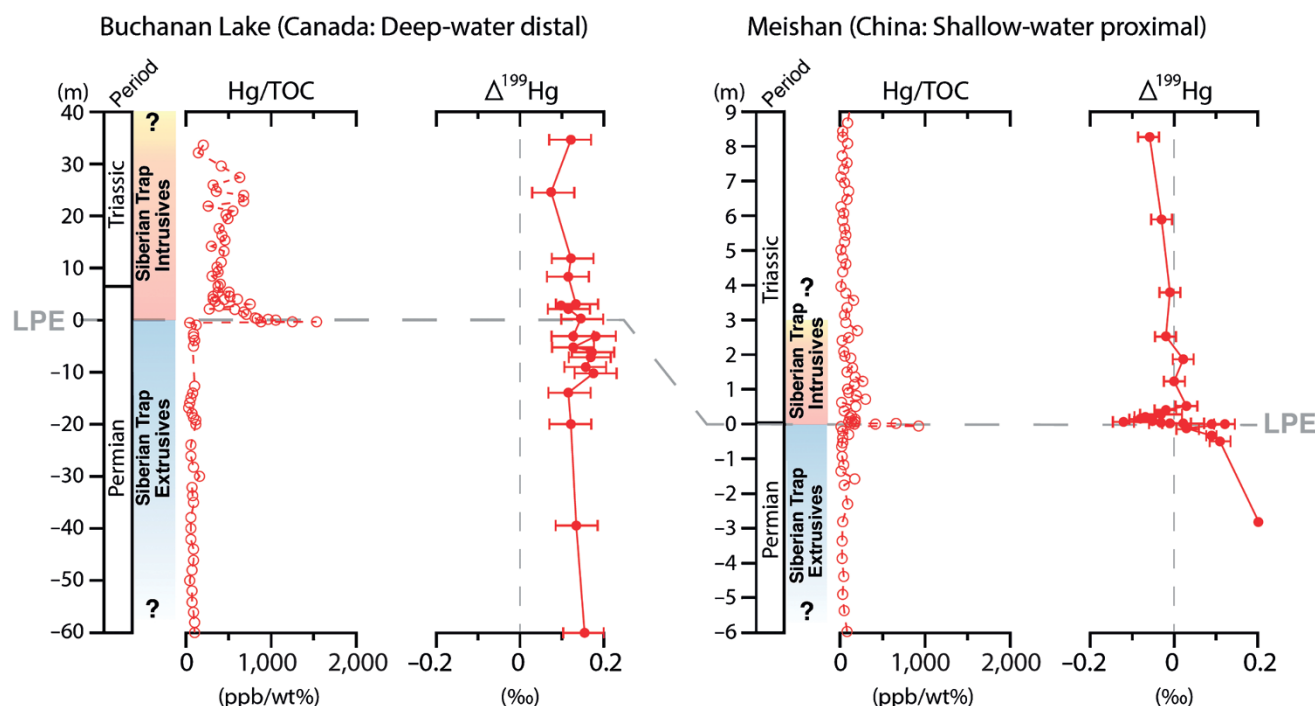


Figure 11.5 Permian-Triassic Hg trends. Hg/TOC and $\Delta^{199}\text{Hg}$ data from Permian-Triassic records of Buchanan Lake (Canada) and Meishan (China), adapted from figures in Grasby et al. (2017) and Wang et al. (2018). Buchanan Lake temporal information and mercury data are from Grasby et al. (2017); Meishan temporal information and mercury data are from Grasby et al. (2017) and Wang et al. (2018). Siberian Trap geochronology with respect to the Permian–Triassic extinction is from Burgess and Bowring (2015).

when LIP volcanism results in major Hg-cycle perturbations (see discussion in Percival et al., 2018). Thus, while Hg/TOC peaks likely do not record all volcanic events associated with LIP volcanism, they may potentially indicate the times of major volcanogenic volatile release.

11.2.4. Can Hg Isotopes Indicate That Sedimentary Hg Enrichments Are Volcanically Derived?

In addition to correlations of Hg/TOC peaks with other volcanic markers, Hg-isotope studies are being increasingly employed as a tool to identify a volcanic fingerprint of mercury versus other potential sources of Hg influx. Thibodeau et al. (2016) reported $\Delta^{199}\text{Hg}$ within error of zero that correlated with elevated Hg contents and Hg/TOC ratios across Triassic–Jurassic interval strata, hypothesized to result from a huge influx of volcanic mercury (i.e., devoid of MIF, see Introduction and Fig. 11.2) that had overwhelmed the normal pathways taken by the element to reach sediments.

It is interesting that, in contrast to the aforementioned end-Triassic study, Hg-isotope records of the end-Ordovician, end-Permian, Toarcian, and end-Cretaceous events do not show zero MIF correlative with sedimentary Hg enrichments (Sial et al., 2016; Gong et al., 2017;

Grasby et al., 2017; Them et al., 2019; Wang et al., 2018). For records of these events, stratigraphic archives deposited relatively proximally to land tend to display shifts toward more negative MIF values that have been interpreted as a large influx of terrestrial Hg from a nearby land mass, which are sometimes correlative with elevations in Hg/TOC ratios (e.g., Grasby et al., 2017) (Fig. 11.5), although not always perfectly so (e.g., Them et al., 2019). In contrast, many of the studied marine records document slightly positive $\Delta^{199}\text{Hg}$ values throughout the studied stratigraphic sequences, which as described above are likely indicative of photochemical reduction during/after atmospheric deposition of Hg to the marine realm. The continuation of such photochemical reduction despite the increased influx of Hg to these records (suggested by correlative Hg/TOC peaks) highlights the durability of this MIF pathway. Thus, a Hg/TOC peak correlative with positive MIF could be indicative of a substantial rise in atmospheric Hg content, possibly resulting from volcanogenic outgassing. In uppermost Permian sections, there is a clear pattern of the records closest to land documenting negative MIF, while more distally deposited records feature positive MIF, and Hg enrichments were observed at all locations (Grasby et al., 2017; Wang et al., 2018). Taken together, these records support an increase

in the global Hg inventory during the end-Permian mass extinction, but suggest that the normal pathways present in biogeochemical cycling and MIF of mercury were largely maintained, although potentially intensified by the elevated Hg abundance at the Earth's surface during that time.

While there are still relatively few published Hg-isotope data sets from geological records where Hg/TOC peaks have been used to infer volcanic activity, the majority of those Hg-isotope trends do not appear to directly record the original volcanic source, assuming that LIPs emitted Hg devoid of MIF as proposed on the basis of the single study of a modern arc volcano (Zambardi et al., 2009). Rather, Hg isotopes appear to be sensitive to the different pathways taken by Hg to reach sediments deposited proximally or distally to the paleoshoreline (Grasby et al., 2017; Thibodeau & Bergquist, 2017; Bergquist, 2017). However, the use of Hg-isotopes to reconstruct these pathways could still be useful for interpreting how the overall Hg cycle was perturbed. In addition, with a better understanding of MDF, the combined interpretation of MIF and MDF shifts may also help to indicate changes in sources to the global Hg pool.

11.3. SUMMARY

Mercury enrichments have been documented in sedimentary records of all five major mass extinctions and several other episodes of environmental perturbation that occurred during the Phanerozoic. These studies indicate that the mercury cycle was perturbed, at least on a regional scale, during all of those events. As volcanism is a major natural source of mercury to the Earth's surface, and sediments the ultimate (and geologically rapid) sink, it appears that mercury may show significant promise as a sedimentary proxy for large-scale volcanic activity. The correlation between mercury enrichments and reconstructed increases in other volcanic gases during at least two major events associated with volcanism supports this possibility. Furthermore, the absence of such elevated Hg concentrations in strata that record times not associated with major volcanism lends further credence to the influence of large-scale volcanic eruptions on the global mercury cycle. At the present time, mercury isotopes appear to be a good indicator of pathways taken by mercury (of whatever origin) to reach the sediment, but may not always record an original volcanic source. However, knowledge of these pathways may nonetheless allow more accurate reconstruction of a mercury cycle perturbation and whether any increases in the global inventory were caused directly by volcanogenic processes or by output from other reservoirs such as biomass, soils, and coal.

However, it is also apparent that there are a number of complexities associated with the use of the mercury proxy that remain to be fully understood. Even if an increase to the global mercury inventory is indicated by a broadly correlative enrichment in sedimentary mercury levels from numerous stratigraphic archives across multiple continents, spatial variability in the global signature will inevitably result from sedimentological and/or depositional processes specific to individual environments, as well as the nature of the volcanism itself. And in some cases, those same sedimentological/volcanological controls will mean that a Hg-cycle perturbation might not be recorded at all in some stratigraphic archives, potentially meaning that any Hg enrichment cannot be globally correlated. The clear lack of correlation between mercury enrichments and other geochronological and/or geochemical evidence for Large Igneous Province volcanism is suggestive that not all eruptive events will manifestly result in a major output of mercury to the environment, certainly on a global scale, and possibly even locally to the Province. Finally, there is also the potential for other Earth surface processes, such as increased runoff of soil/plant material, to elevate the flux of Hg to sediments on a local or possibly global scale. Although such an input may also simply reflect intense recycling of originally volcanic mercury, and global-scale increases in weathering rates are typically associated with times of large-scale volcanism. In short, it is essential to study multiple sites covering different facies in order to gain a clearer overview of the global mercury cycle, which will not necessarily be represented within every single sedimentary record or even an individual large geographical region. Future work should focus on exploring the many nuances of sedimentary mercury in order to better understand the element as a proxy for volcanism, investigating how mercury isotopes can be best employed in understanding past mercury perturbations, and confirming whether those disturbances were global or regional in extent during different Phanerozoic events by expanding the geographical distribution of stratigraphic records studied for mercury.

ACKNOWLEDGMENTS

Numerous past and present members of the Stratigraphy and Sedimentology research groups in Oxford and Lausanne are thanked for helpful discussions related to this topic, especially Hugh Jenkyns, Alex Dickson, Steve Hesselbo, Micha Ruhl, and Guillaume Charbonnier. We also gratefully acknowledge the NSERC Discovery (RGPIN-2018-06569 to B.A.B.) and the Research Foundation, Flanders (FWO), and University of Lausanne (to L.M.E.P) for financial support.

REFERENCES

- Bacon, K. L., Belcher, C. M., Haworth, M., & McElwain, J. C. (2013). Increased atmospheric SO₂ detected from changes in leaf physiognomy across the Triassic-Jurassic boundary interval of east Greenland. *PLoS ONE*, 8, e60614. <https://doi.org/10.1371/journal.pone.0060614>
- Bagnato, E., Aiuppa, A., Parello, F., Allard, P., Shinohara, H., Liuzzo, F., & Giudice, G. (2011). New clues on the contribution of Earth's volcanism to the global mercury cycle. *Bulletin of Volcanology*, 73, 497–510. <https://doi.org/10.1007/s00445-010-0419-y>
- Bagnato, E., Aiuppa, A., Parello, F., Calabrese, S., D'Alessandro, W., Mather, T. A., McGonigle, A. J. S., et al. (2007). Degassing of gaseous (elemental and reactive) and particulate mercury from Mount Etna volcano (Southern Italy). *Atmospheric Environment*, 41, 7377–7388. <https://doi.org/10.1016/j.atmosenv.2007.05.060>
- Bagnato, E., Tamburello, G., Avaró, G., Martínez-Cruz, M., Enrico, M., Ful, X., Sprovieri, M., et al. (2014). Mercury fluxes from volcanic and geothermal sources: An update. *Geological Society, London, Special Publications*, 410. <https://doi.org/10.1144/SP410.2>
- Bergquist, B. A. (2017). Mercury, volcanism, and mass extinctions. *Proceedings of the National Academy of Sciences*, 114, 8675–8677. <https://doi.org/10.1073/pnas.1709070114>
- Bergquist, B. A., & Blum, J. D. (2007). Mass-dependent and independent fractionation of Hg isotopes by photoreduction in aquatic systems. *Science*, 318, 417–420. <https://doi.org/10.1126/science.1148050>
- Blackburn, T. J., Olsen, P. E., Bowring, S. A., McLean, N. M., Kent, D. V., Puffer, J., McHone, G., et al. (2013). Zircon U-Pb geochronology links the end-Triassic extinction with the Central Atlantic Magmatic Province. *Science*, 340, 941–945. <https://doi.org/10.1126/science.1234204>
- Blum, J. D., Sherman, L. S., & Johnson, M. W. (2014). Mercury isotopes in earth and environmental sciences. *Annual Review of Earth and Planetary Sciences*, 42, 249–269. <https://doi.org/10.1146/annurev-earth-050212-124107>
- Bond, D. P., & Wignall, P. B. (2014). Large igneous provinces and mass extinctions: An update. *Geological Society of America Special Papers*, 505, SPE505-02. [https://doi.org/10.1130/2014.2505\(02\)](https://doi.org/10.1130/2014.2505(02))
- Bowman, K. L., Hammerschmidt, C. R., Lamborg, C. H., & Swarr, G. (2015). Mercury in the North Atlantic Ocean: The U.S. GEOTRACES zonal and meridional sections. *Deep-Sea Research II*, 116, 251–261. <https://doi.org/10.1016/j.dsr2.2014.07.004>
- Burger, B. J., Estrada, M. V., & Gustin, M. S. (2019). What caused Earth's largest mass extinction event? New evidence from the Permian-Triassic boundary in northeastern Utah. *Global and Planetary Change*, 177, 81–100. <https://doi.org/10.1016/j.gloplacha.2019.03.013>
- Burgess, S. D., & Bowring, S. A. (2015). High-precision geochronology confirms voluminous magmatism before, during, and after Earth's most severe extinction. *Science Advances*, 1, e1500470. <https://doi.org/10.1126/sciadv.1500470>
- Carignan, J., Estrade, N., Sonke, J. E., & Donard, O. F. (2009). Odd isotope deficits in atmospheric Hg measured in lichens. *Environmental Science & Technology*, 43, 5660–5664. <https://doi.org/10.1021/es900578v>
- Charbonnier, G., & Föllmi, K. B. (2017). Mercury enrichments in lower Aptian sediments support the link between Ontong Java large igneous province activity and oceanic anoxic episode 1a. *Geology*, 45, 63–66. <https://doi.org/10.1130/G38207.1>
- Charbonnier, G., Adatte, T., Duchamp-Alphonse, S., Spangenberg, J. E., & Föllmi, K. B. (in press). *Global mercury enrichment in Valanginian sediments supports a volcanic trigger for the Weissert episode*. Geological Society of America Special Papers, 544, SPE544-04. [https://doi.org/10.1130/2019.2544\(04\)](https://doi.org/10.1130/2019.2544(04))
- Charbonnier, G., Adatte, T., Föllmi, K. B., & Suan, G. (2020). Effect of intense weathering and post-depositional degradation of organic matter on Hg/TOC proxy in organic-rich sediments and its implications for deep-time investigations. *Geochemistry, Geophysics, Geosystems*. <https://doi.org/10.1029/2019GC008707>
- Charbonnier, G., Godet, A., Bodin, S., Adatte, T., & Föllmi, K. B. (2018). Mercury anomalies, volcanic pulses, and drowning episodes along the northern Tethyan margin during the latest Hauterivian-earliest Aptian. *Palaeogeography, Palaeoclimatology, Palaeoecology*, 15, 337–350. <https://doi.org/10.1016/j.palaeo.2018.06.013>
- Charbonnier, G., Morales, C., Duchamp-Alphonse, S., Westermann, S., Adatte, T., & Föllmi, K. B. (2017). Mercury enrichment indicates volcanic triggering of Valanginian environmental change. *Scientific Reports*, 7. <https://doi.org/10.1038/srep40808>
- Courtillot, V., & Renne, P. R. (2003). On the ages of flood basalt events. *Comptes Rendus Geoscience*, 335, 113–140. [https://doi.org/10.1016/S1631-0713\(03\)00006-3](https://doi.org/10.1016/S1631-0713(03)00006-3)
- Daga, R., Guevara, S. R., Pavlin, M., Rizzo, A., Lojen, S., Vreča, P., Horvat, M., & Arribé, M. (2016). Historical records of mercury in southern latitudes over 1600 years: Lake Futalaufquen, Northern Patagonia. *Science of the Total Environment*, 553, 541–550. <https://doi.org/10.1016/j.scitotenv.2016.02.114>
- Davies, J. H. F. L., Marzoli, A., Bertrand, H., Youbi, N., Ernesto, M., & Schaltegger, U. (2017). End-Triassic mass extinction started by intrusive CAMP activity. *Nature Communications*, 8. <https://doi.org/10.1038/ncomms15596>
- Demers, J. D., Blum, J. D., & Zak, D. R. (2013). Mercury isotopes in a forested ecosystem: Implications for air-surface exchange dynamics and the global mercury cycle. *Global Biogeochemical Cycles*, 27, 222–238. <https://doi.org/10.1002/gbc.20021>
- Du Vivier, A. D. C., Selby, D., Sageman, B. B., Jarvis, I., Gröcke, D. R., & Voigt, S. (2014). Marine ¹⁸⁷Os/¹⁸⁸Os isotope stratigraphy reveals the interaction of volcanism and ocean circulation during Oceanic Anoxic Event 2. *Earth and Planetary Science Letters*, 389, 23–33. <https://doi.org/10.1016/j.epsl.2013.12.024>
- Du Vivier, A. D. C., Selby, D., Takashima, R., & Nishi, H. (2015). Pacific ¹⁸⁷Os/¹⁸⁸Os isotope geochemistry and U-Pb geochronology: Synchronicity of global Os isotope change across OAE 2. *Earth and Planetary Science Letters*, 428, 204–216. <https://doi.org/10.1016/j.epsl.2015.07.020>
- Eddy, M. P., Schoene, B., Samperton, K. M., Keller, G., Adatte, T., & Khadri, S. F. (2020). U-Pb zircon age constraints on the earliest eruptions of the Deccan Large Igneous Province, Malwa Plateau, India. *Earth and Planetary Science Letters*, 540, 116249. <https://doi.org/10.1016/j.epsl.2020.116249>

- Enrico, M., Roux, G. L., Maruszczak, N., Heimbürger, L. E., Claustres, A., Fu, X., Sun, R., & Sonke, J. E. (2016). Atmospheric mercury transfer to peat bogs dominated by gaseous elemental mercury dry deposition. *Environmental Science & Technology*, 50, 2405–2412. <https://doi.org/10.1021/acs.est.5b06058>
- Ericksen, J. A., Gustin, M. S., Schorran, D. E., Johnson, D. W., Lindberg, S. E., & Coleman, J. S. (2003). Accumulation of atmospheric mercury in forest foliage. *Atmospheric Environment*, 36, 1613–1622. [https://doi.org/10.1016/S1352-2310\(03\)00008-6](https://doi.org/10.1016/S1352-2310(03)00008-6)
- Faggetter, L. E., Wignall, P. B., Pruss, S. B., Jones, D. S., Grasby, S., Widdowson, M., & Newton, R. J. (2019). Mercury chemostratigraphy across the Cambrian Series 2-Series 3 boundary: evidence for increased volcanic activity coincident with extinction? *Chemical Geology*, 510, 188–199. <https://doi.org/10.1016/j.chemgeo.2019.02.006>
- Fantasia, A., Adatte, T., Spangenberg, J. E., Font, E., Duarte, L. V., & Föllmi, K. B. (2019). Global versus local processes during the Pliensbachian-Toarcian transition at the Peniche GSSP, Portugal: A multi-proxy record. *Earth-Science Reviews*. <https://doi.org/10.1016/j.earscirev.2019.102932>
- Fantasia, A., Föllmi, K. B., Adatte, T., Bernárdez, E., Spangenberg, J. E., & Mattioli, E. (2018). The Toarcian Oceanic Anoxic Event in southwestern Gondwana: An example from the Andean Basin, northern Chile. *Journal of the Geological Society (London)*. <https://doi.org/10.1144/jgs2018-008>
- Fendley, I. M., Mittal, T., Sprain, C. J., Marvin-DiPasquale, M., Tobin, T. S., & Renne, P. R. (2019). Constraints on the volume and rate of Deccan Traps flood basalt eruptions using a combination of high-resolution terrestrial mercury records and geochemical box models. *Earth and Planetary Science Letters*, 524. <https://doi.org/10.1016/j.epsl.2019.115721>
- Fitzgerald, W. F., & Lamborg, C. H. (2014). Geochemistry of mercury in the environment. In H. Holland & K. Turekian (Eds.), *Treatise on geochemistry* (2nd ed.) (pp. 91–129). Oxford: Elsevier.
- Fitzgerald, W. F., Lamborg, C. H., & Hammerschmidt, C. R. (2007). Marine biogeochemical cycling of mercury. *Chemical Reviews*, 107, 641–662. <https://doi.org/10.1021/cr050353m>
- Font, E., Adatte, T., Andrade, M., Keller, G., Bitchong, A. M., Carvallo, C., Ferreira, J., et al. (2018). Deccan volcanism induced high-stress environment during the Cretaceous-Paleogene transition at Zumaia, Spain: Evidence from magnetic, mineralogical and biostratigraphic records. *Earth and Planetary Science Letters*, 484, 53–66. <https://doi.org/10.1016/j.epsl.2017.11.055>
- Font, E., Adatte, T., Sial, A. N., de Lacerda, L. D., Keller, G., & Punekar, J. (2016). Mercury anomaly, Deccan volcanism, and the end-Cretaceous mass extinction. *Geology*, 44, 171–174. <https://doi.org/10.1130/G37451.1>
- Ganino, C., & Arndt, N. T. (2009). Climate changes caused by degassing of sediments during the emplacement of large igneous provinces. *Geology*, 37, 323–326. <https://doi.org/10.1130/G25325A.1>
- Gehrke, G. E., Blum, J. D., & Meyers, P. A. (2009). The geochemical behavior and isotopic composition of Hg in a mid-Pleistocene western Mediterranean sapropel. *Geochimica et Cosmochimica Acta*, 73, 1651–1665. <https://doi.org/10.1016/j.gca.2008.12.012>
- Gill, G. A., & Fitzgerald, W. F. (1988). Vertical mercury distributions in the oceans. *Geochimica et Cosmochimica Acta*, 52, 1719–1728. [https://doi.org/10.1016/0016-7037\(88\)90240-2](https://doi.org/10.1016/0016-7037(88)90240-2)
- Gong, Q., Wang, X., Zhao, L., Grasby, S. E., Chen, Z. Q., Zhang, L., Li, Y., et al. (2017). Mercury spikes suggest volcanic driver of the Ordovician-Silurian mass extinction. *Scientific Reports*, 7. <https://doi.org/10.1038/s41598-017-05524-5>
- Grasby, S. E., Beauchamp, B., Bond, D. P. G., Wignall, P., & Sanei, H. (2016). Mercury anomalies associated with three extinction events (Capitanian Crisis, Latest Permian Extinction and the Smithian/Spathian Extinction) in NW Pangea. *Geological Magazine*, 153, 285–297. <https://doi.org/10.1017/S0016756815000436>
- Grasby, S. E., Beauchamp, B., Embry, A., & Sanei, H. (2013a). Recurrent Early Triassic ocean anoxia. *Geology*, 41, 175–178. <https://doi.org/10.1130/G33599.1>
- Grasby, S. E., Sanei, H., Benoit, B., & Chen, Z. (2013b). Mercury deposition through the Permo-Triassic Biotic Crisis. *Chemical Geology*, 351, 209–216. <https://doi.org/10.1016/j.chemgeo.2013.05.022>
- Grasby, S. E., Them, T. R., Chen, Z., Yin, R., & Ardakani, O. H. (2019). Mercury as a proxy for volcanic emissions in the geologic record. *Earth Science Reviews*, 196. <https://doi.org/10.1016/j.earscirev.2019.102880>
- Grasby, S. E., Wenjie, S., Runsheng, Y., Gleason, J. D., Blum, J. D., Lepak, R. F., Hurley, J. P., et al. (2017). Isotopic signatures of mercury contamination in latest Permian oceans. *Geology*, 45, 55–58. <https://doi.org/10.1130/G38487.1>
- Gustin, M. S., Amos, H. M., Huang, J., Miller, M. B., & Heidecorn, K. (2015). Measuring and modeling mercury in the atmosphere: a critical review. *Atmospheric Chemistry and Physics*, 15, 5697–5713. <https://doi.org/10.5194/acp-15-5697-2015>
- Hammer, Ø., Jones, M. T., Schneebeli-Hermann, E., Hansen, B. B., & Bucher, H. (2019). Are Early Triassic extinction events associated with mercury anomalies? A reassessment of the Smithian/Spathian boundary extinction. *Earth-Science Reviews*, 195, 179–190. <https://doi.org/10.1016/j.earscirev.2019.04.016>
- Hesselbo, S. P., Gröcke, D. R., Jenkyns, H. C., Bjerrum, C. J., Farrimond, P. L., Morgans-Bell, H. S., & Green, O. (2000). Massive dissociation of gas hydrates during a Jurassic Oceanic Anoxic Event. *Nature*, 406, 392–395. <https://doi.org/10.1038/35019044>
- Hesselbo, S. P., Robinson, S. A., Surlyk, F., & Piasecki, S. (2002). Terrestrial and marine extinction at the Triassic-Jurassic boundary synchronized with major carbon-cycle perturbation: A link to initiation of massive volcanism? *Geology*, 30, 251–254. [https://doi.org/10.1130/0091-7613\(2002\)030<0251:TAMEAT>2.0.CO;2](https://doi.org/10.1130/0091-7613(2002)030<0251:TAMEAT>2.0.CO;2)
- Jin, H., & Liebezeit, G. (2013). Distribution of total mercury in coastal sediments from Jade Bay and its catchment, Lower Saxony, Germany. *Journal of Soils and Sediments*, 13, 441–449. <https://doi.org/10.1007/s11368-012-0626-6>
- Jones, D. S., Martini, A. M., Fike, D. A., & Kaiho, K. (2017). A volcanic trigger for the Late Ordovician mass extinction? Mercury data from south China and Laurentia. *Geology*, 45, 631–634. <https://doi.org/10.1130/G38940.1>

- Jones, M. T., Percival, L. M. E., Stokke, E. W., Frieling, J., Mather, T. A., Riber, L., Schubert, B. A., et al. (2019). Mercury anomalies across the Paleocene-Eocene Thermal Maximum. *Climate of the Past*, 15. <https://doi.org/10.5194/cp-15-217-2019>
- Kalvoda, J., Kumpan, T., Qie, W., Frýda, J., & Bábek, O. (2019). Mercury spikes at the Devonian-Carboniferous boundary in the eastern part of the Rhenohercynian Zone (central Europe) and in the South China Block. *Palaeogeography, Palaeoclimatology, Palaeoecology*, 531. <https://doi.org/10.1016/j.palaeo.2019.05.043>
- Keller, G., Mateo, P., Punekar, J., Khozyem, H., Gertsch, B., Spangenberg, J., Bitchong, A., et al. (2018). Environmental changes during the Cretaceous-Paleogene mass extinction and Paleocene-Eocene thermal maximum: Implications for the Anthropocene. *Gondwana Research*, 56, 69–89. <https://doi.org/10.1016/j.gr.2017.12.002>
- Kwon, H., Kim, M. G., & Lee, Y. I. (2018). Mercury evidence from the Sino-Korean block for Emeishan volcanism during the Capitanian mass extinction. *Geological Magazine*, 1–6. <https://doi.org/10.1017/S0016756818000481>
- Lamborg, C. H., Von Damm, K. L., Fitzgerald, W. F., Hammerschmidt, C. R., & Zierenberg, R. (2006). Mercury and monomethylmercury in fluids from Sea Cliff submarine hydrothermal field, Gorda Ridge. *Geophysical Research Letters*, 33, L17606. <https://doi.org/10.1029/2006GL026321>
- Lindberg, S. E., Hanson, P. J., Meyers, T. A., & Kim, K. H. (1998). Air/surface exchange of mercury vapor over forests: The need for a reassessment of continental biogenic emissions. *Atmospheric Environment*, 32, 895–908. [https://doi.org/10.1016/S1352-2310\(97\)00173-8](https://doi.org/10.1016/S1352-2310(97)00173-8)
- Lindström, S., Sanei, H., Van De Schootbrugge, B., Pedersen, G. K., Leshner, C. E., Tegner, C., Heunisch, C., et al. (2019). Volcanic mercury and mutagenesis in land plants during the end-Triassic mass extinction. *Science Advances*, 5. <https://doi.org/10.1126/sciadv.aaw4018>
- Liu, X., Xu, L., Chen, Q., Sun, L., Wand, Y., Yan, H., Liu, Y., Luo, Y., & Huang, J. (2012). Historical change of mercury pollution in remote Yongle archipelago, South China Sea. *Chemosphere*, 87, 549–556. <https://doi.org/10.1016/j.chemosphere.2011.12.065>
- Liu, Z., Horton, D. E., Tabor, C., Sageman, B. B., Percival, L. M. E., Gill, B. C., & Selby, D. (2019). Assessing the contributions of comet impact and volcanism towards the climate perturbations of the Paleocene-Eocene Thermal Maximum. *Geophysical Research Letters*. <https://doi.org/10.1029/2019GL084818>
- Mander, L., Kürschner, W. M., & McElwain, J. C. (2013). Palynostratigraphy and vegetation history of the Triassic-Jurassic transition in East Greenland. *Journal of the Geological Society*, 170, 37–46. <https://doi.org/10.1144/jgs2012-018>
- McElwain, J. C., Wade-Murphy, J., & Hesselbo, S. P. (2005). Changes in carbon dioxide during an oceanic anoxic event linked to intrusion into Gondwana coals. *Nature*, 435, 479–482. <https://doi.org/10.1038/nature03618>
- Meyer, K. W., Petersen, S. V., Lohmann, K. C., Blum, J. D., Washburn, S. J., Johnson, M. W., Gleason, J. D., et al. (2019). Biogenic carbonate mercury and marine temperature records reveal global influence of Late Cretaceous Deccan Traps. *Nature Communications*, 10. <https://doi.org/10.1038/s41467-019-13366-0>
- Morgans-Bell, H. S., Coe, A. L., Hesselbo, S. P., Jenkyns, H. C., Weedon, G. P., Marshall, J. E. A., Tyson, R. V., et al. (2001). Integrated stratigraphy of the Kimmeridge Clay Formation (Upper Jurassic) based on exposures and boreholes in south Dorset, UK. *Geological Magazine*, 138(5), 511–539. <https://doi.org/10.1017/S0016756801005738>
- Obrist, D. (2007). Atmospheric mercury pollution due to losses of terrestrial carbon pools? *Biogeochemistry*, 85, 119–123. <https://doi.org/10.1007/s10533-007-9108-0>
- Obrist, D., Johnson, D. W., Lindberg, S. E., Luo, Y., Hararuk, O., Bracho, R., Battles, J. J., et al. (2011). Mercury distribution across 14 US forests. Part I: Spatial patterns of concentrations in biomass, litter, and soils. *Environmental Science & Technology*, 45, 3974–3981. <https://doi.org/10.1021/es104384m>
- Obrist, D., Kirk, J. L., Zhang, L., Sunderland, E. M., Jiskra, M., & Selin, N. E. (2018). A review of global environmental mercury processes in response to human and natural perturbations: Changes of emissions, climate, and land use. *Ambio*, 47, 116–140. <https://doi.org/10.1007/s13280-017-1004-9>
- Outridge, P. M., Sanei, H., Stern, G. A., Hamilton, P. B., & Goodarzi, F. (2007). Evidence for control of mercury accumulation in sediments by variations of aquatic primary productivity in Canadian High Arctic lakes. *Environmental Science and Technology*, 41, 5259–5265. <https://doi.org/10.1021/es070408x>
- Paschall, O., Carmichael, S. K., Königshof, P., Waters, J. A., Ta, P. H., Komatsu, T., & Dombrowski, A. (2019). The Devonian-Carboniferous boundary in Vietnam: Sustained ocean anoxia with a volcanic trigger for the Hangenberg Crisis? *Global and Planetary Change*, 175, 64–81. <https://doi.org/10.1016/j.gloplacha.2019.01.021>
- Percival, L. M. E., Jenkyns, H. C., Mather, T. A., Dickson, A. J., Batenburg, S. J., Ruhl, M., Hesselbo, S. P., et al. (2018). Does Large Igneous Province volcanism always perturb the mercury cycle? Comparing the records of Oceanic Anoxic Event 2 and the end-Cretaceous to other Mesozoic events. *American Journal of Science*, 318, 799–860. <https://doi.org/10.2475/08.2018.01>
- Percival, L. M. E., Ruhl, M., Hesselbo, S. P., Jenkyns, H. C., Mather, T. M., & Whiteside, J. H. (2017). Mercury evidence for pulsed volcanism during the end-Triassic mass extinction. *Proceedings of the National Academy of Sciences of the United States of America*, 114, 7929–7934. <https://doi.org/10.1073/pnas.1705378114>
- Percival, L. M. E., Witt, M. L. I., Mather, T. A., Hermoso, M., Jenkyns, H. C., Hesselbo, S. P., Al-Suwaidi, A. H., et al. (2015). Globally enhanced mercury deposition during the end-Pliensbachian extinction and Toarcian OAE: A link to the Karoo-Ferrar Large Igneous Province. *Earth and Planetary Science Letters*, 428, 267–280. <https://doi.org/10.1016/j.epsl.2015.06.064>
- Pruss, S. B., Jones, D. S., Fike, D. A., Tosca, N. J., & Wignall, P. B. (2019). Marine anoxia and sedimentary mercury enrichments during the Late Cambrian SPICE event in northern Scotland. *Geology*. <https://doi.org/10.1130/G45871.1>
- Pyle, D. M., & Mather, T. A. (2003). The importance of volcanic emissions for the global atmospheric mercury cycle. *Atmospheric Environment*, 37, 5115–5124. <https://doi.org/10.1016/j.atmosenv.2003.07.011>

- Racki, G., Rakociński, M., & Marynowski, L. (2018b). Anomalous Upper Devonian mercury enrichments: comparison of Inductively Coupled Plasma-Mass Spectrometry (ICP-MS) and Atomic Absorption Spectrometry (AAS) analytical data. *Geological Quarterly*, 62, 487–495. <https://doi.org/10.7306/gq.1419>
- Racki, G., Rakociński, M., Marynowski, L., & Wignall, P. B. (2018a). Mercury enrichments and the Frasnian-Famennian biotic crisis: A volcanic trigger proved? *Geology*. <https://doi.org/10.1130/G40233.1>
- Rampino, M. R., & Strothers, R. B. (1988). Flood basalt volcanism during the past 250 million years. *Science*, 241, 663–668. <https://doi.org/10.1126/science.241.4866.663>
- Ravizza, G., & Peucker-Ehrenbrink, B. (2003). Chemostratigraphic evidence of Deccan volcanism from the marine osmium isotope record. *Science*, 302, 1392–1395. <https://doi.org/10.1126/science.1089209>
- Renne, P. R., Sprain, C. J., Richards, M. A., Self, S., Vanderkluyzen, L., & Pande, K. (2015). State shift in Deccan volcanism at the Cretaceous-Paleogene boundary, possibly induced by impact. *Science*, 350, 76–78. <https://doi.org/10.1126/science.aac7549>
- Ribeiro Guevara, S., Meili, M., Rizzo, A., Daga, R., & Arribère, M. (2010). Sediment records of highly variable mercury inputs to mountain lakes in Patagonia during the past millennium. *Atmospheric Chemistry and Physics*, 10, 3443–3453. <https://doi.org/10.5194/acp-10-3443-2010>
- Robinson, N., Ravizza, G., Coccioni, R., Peucker-Ehrenbrink, B., & Norris, R. (2009). A high-resolution marine $^{187}\text{Os}/^{188}\text{Os}$ record for the late Maastrichtian: Distinguishing the chemical fingerprints of Deccan volcanism and the KP impact event. *Earth and Planetary Science Letters*, 281, 159–168. <https://doi.org/10.1016/j.epsl.2009.02.019>
- Ruiz, W. L. G., & Tomiyasu, T. (2015). Distribution of mercury in sediments from Kagoshima Bay, Japan, and its relationship with physical and chemical factors. *Environmental Earth Sciences*, 74, 1175–1188. <https://doi.org/10.1007/s12665-015-4104-5>
- Sabatino, N., Ferraro, S., Coccioni, R., Bonsignore, M., Del Core, M., Tancredi, V., & Sprovieri, M., (2018). Mercury anomalies in upper Aptian-lower Albian sediments from the Tethys realm. *Palaeogeography, Palaeoclimatology, Palaeoecology*, 495, 163–170. <https://doi.org/10.1016/j.palaeo.2018.01.008>
- Sanei, H., & Goodarzi, F., 2006, Relationship between organic matter and mercury in recent lake sediment: the physical-geochemical aspects. *Applied Geochemistry*, 21, 1900–1912. <https://doi.org/10.1016/j.apgeochem.2006.08.015>
- Sanei, H., Grasby, S., & Beauchamp, B. (2012). Latest Permian mercury anomalies. *Geology*, 40, 63–66. <https://doi.org/10.1130/G32596.1>
- Sanei, H., Outridge, P. M., Stern, G. A., & Macdonald, R. W. (2014). Classification of mercury-labile organic matter relationships in lake sediments. *Chemical Geology*, 373, 87–92. <https://doi.org/10.1016/j.chemgeo.2014.02.029>
- Scaife, J. D., Ruhl, M., Dickson, A. J., Mather, T. A., Jenkyns, H. C., Percival, L. M. E., Hesselbo, S. P., et al. (2017). Sedimentary mercury enrichments as a marker for submarine Large Igneous Province volcanism? Evidence from the Mid-Cenomanian Event and Oceanic Anoxic Event 2 (Late Cretaceous). *Geochemistry, Geophysics, Geosystems*, 18, 4253–4275. <https://doi.org/10.1002/2017GC007153>
- Schoene, B., Samperton, K. M., Eddy, M. P., Keller, G., Adatte, T., Bowring, S. A., Khadri, S. F., & Gertsch, B. (2015). U-Pb geochronology of the Deccan Traps and relation to the end-Cretaceous mass extinction. *Science*, 347, 182–184. <https://doi.org/10.1126/science.aaa0118>
- Schoene, B., Eddy, M.P., Samperton, K.M., Keller, C.B., Keller, G., Adatte, T. and Khadri, S.F. (2019). U-Pb constraints on pulsed eruption of the Deccan Traps across the end-Cretaceous mass extinction. *Science*, 363, 862–866. <https://doi.org/10.1126/science.aau2422>
- Schroeder, W. H., & Munthe, J. (1998). Atmospheric mercury: An overview. *Atmospheric Environment*, 32, 809–822. [https://doi.org/10.1016/S1352-2310\(97\)00293-8](https://doi.org/10.1016/S1352-2310(97)00293-8)
- Selin, N. E. (2009). Global biogeochemical cycling of mercury: A review. *Annual Review of Environment and Resources*, 34, 43–63. <https://doi.org/10.1146/annurev.enviro.051308.084314>
- Sell, B., Ovtcharova, M., Guex, J., Bartolini, A., Jourdan, F., Spangenberg, J. E., Vicente, J. C., et al. (2014). Evaluating the temporal link between the Karoo LIP and climatic-biologic events of the Toarcian stage with high-precision U-Pb geochronology. *Earth and Planetary Science Letters*, 408, 48–56. <https://doi.org/10.1016/j.epsl.2014.10.008>
- Shen, J., Algeo, T. J., Chen, J., Planavski, N. J., Feng, Q., Yu, J., & Liu, J. (2019b). Mercury in marine Ordovician/Silurian boundary sections of South China is sulfide-hosted and non-volcanic in origin. *Earth and Planetary Science Letters*, 511, 130–140. <https://doi.org/10.1016/j.epsl.2019.01.028>
- Shen, J., Algeo, T. J., Planavsky, N. J., Yu, J., Feng, Q., Song, H., Song, H., et al. (2019a). Mercury enrichments provide evidence of Early Triassic volcanism following the end-Permian mass extinction. *Earth-Science Reviews*, 195, 191–212. <https://doi.org/10.1016/j.earscirev.2019.05.010>
- Shen, J., Chen, J., Algeo, T. J., Yuan, S., Feng, Q., Yu, J., Zhou, L., O'Connell, B., Planavsky, N. J. (2019c). Evidence for a prolonged Permian-Triassic extinction interval from global marine mercury records. *Nature Communications*, 10. <https://doi.org/10.1038/s41467-019-09620-0>
- Sial, A. N., Chen, J., Lacerda, L. D., Frei, R., Tewari, V. C., Pandit, M. K., Gaucher, C., et al. (2016). Mercury enrichment and Hg isotopes in Cretaceous-Paleogene boundary successions: Links to volcanism and palaeoenvironmental impacts. *Cretaceous Research*, 66, 60–81. <https://doi.org/10.1016/j.cretres.2016.05.006>
- Sial, A. N., Chen, J., Lacerda, L. D., Korte, C., Spangenberg, J. E., Silva-Tamayo, J. C., Gaucher, C., et al. (2020). Globally enhanced Hg deposition and Hg isotopes in sections straddling the Permian-Triassic boundary: Link to volcanism. *Palaeogeography, Palaeoclimatology, Palaeoecology*, 540. <https://doi.org/10.1016/j.palaeo.2019.109537>
- Sial, A. N., Chen, J., Lacerda, L. D., Peralta, S., Gaucher, C., Frei, R., Cirilli, S., et al. (2014). High-resolution Hg chemostratigraphy: A contribution to the distinction of chemical fingerprints of the Deccan volcanism and Cretaceous-Paleogene Boundary impact event. *Palaeogeography, Palaeoclimatology, Palaeoecology*, 414, 98–115. <https://doi.org/10.1016/j.palaeo.2014.08.013>
- Sial, A. N., Lacerda, L. D., Ferreira, V. P., Frei, R., Marquillas, R. A., Barbosa, J. A., Gaucher, C., et al. (2013). Mercury as a proxy for volcanic activity during extreme environmental turnover: The Cretaceous-Paleogene transition. *Palaeogeography,*

- Palaeoclimatology, Palaeoecology*, 387, 153–164. <https://doi.org/10.1016/j.palaeo.2013.07.019>
- Slemr, F., Schuster, G., & Seiler, W. (1985). Distribution, speciation, and budget of atmospheric mercury. *Journal of Atmospheric Chemistry*, 3, 407–434. <https://doi.org/10.1007/BF00053870>
- Smolarek-Lach, J., Marynowski, L., Trela, W., & Wignall, P. B. (2019). Mercury spikes indicate a volcanic trigger for the Late Ordovician mass extinction event: An example from a deep shelf of the Peri-Baltic region. *Scientific Reports*, 9, <https://doi.org/10.1038/s41598-019-39333-9>
- Sonke, J. E. (2011). A global model of mass independent mercury stable isotope fractionation. *Geochimica et Cosmochimica Acta*, 75, 4577–4590. <https://doi.org/10.1016/j.gca.2011.05.027>
- Sprain, C. J., Renne, P. R., Vanderkluisen, L., Pande, K., Self, S., and Mittal, T. (2019). The eruptive tempo of Deccan volcanism in relation to the Cretaceous–Paleogene boundary. *Science*, 363, 866–870. <https://doi.org/10.1126/science.aav1446>
- Steinhorsdottir, M., Elliott-Kingston, C., & Bacon, K. L. (2018). Cuticle surfaces of fossil plants as a potential proxy for volcanic SO₂ emissions: Observations from the Triassic–Jurassic transition of East Greenland. *Palaeobiodiversity and Palaeoenvironments*, 98, 49–69. <https://doi.org/10.1007/s12549-017-0297-9>
- Steinhorsdottir, M., Jeram, A. J., & McElwain, J. C. (2011). Extremely elevated CO₂ concentrations at the Triassic/Jurassic boundary. *Palaeogeography, Palaeoclimatology, Palaeoecology*, 308, 418–432. <https://doi.org/10.1016/j.palaeo.2011.05.050>
- Svensen, H., Corfu, F., Polteau, S., Hammer, Ø., & Planke, S. (2012). Rapid magma emplacement in the Karoo large igneous province. *Earth and Planetary Science Letters*, 325, 1–9. <https://doi.org/10.1016/j.epsl.2012.01.015>
- Svensen, H., Planke, S., Mørth, S., Jamtveit, B., Myklebust, R., Eidem, T. R., & Rey, S. S. (2004). Release of methane from a volcanic basin as a mechanism for initial Eocene global warming. *Nature*, 429, 542–545. <https://doi.org/10.1038/nature02566>
- Svensen, H., Planke, S., Polozov, A. G., Schmidbauer, N., Corfu, F., Podladchikov, Y. Y., & Jamtveit, B. (2009). Siberian gas venting and the end-Permian environmental crisis. *Earth and Planetary Science Letters*, 277, 490–500. <https://doi.org/10.1016/j.epsl.2008.11.015>
- Them, T. R., Jagoe, C. H., Caruthers, A. H., Gill, B. C., Grasby, S. E., Gröcke, D. R., Yin, R., et al. (2019). Terrestrial sources as the primary delivery mechanism of mercury to the oceans across the Toarcian Oceanic Anoxic Event (Early Jurassic). *Earth and Planetary Science Letters*, 507, 62–72. <https://doi.org/10.1016/j.epsl.2018.11.029>
- Thibodeau, A. M., & Bergquist, B. A. (2017). Do mercury isotopes record the signature of massive volcanism in marine sedimentary records? *Geology*, 45, 95–96. <https://doi.org/10.1130/focus012017.1>
- Thibodeau, A. M., Ritterbush, K., Yager, J. A., West, J., Ibarra, Y., Bottjer, D. J., Berelson, W. M., et al. (2016). Mercury anomalies and the timing of biotic recovery following the end-Triassic mass extinction. *Nature Communications*, 7, <https://doi.org/10.1038/ncomms11147>
- Turgeon, S. C., & Creaser, R. A. (2008). Cretaceous oceanic anoxic event 2 triggered by a massive magmatic episode. *Nature*, 454, 323–326. <https://doi.org/10.1038/nature07076>
- Wang, X., Bao, Z., Lin, C. J., Yuan, W., & Feng, X. (2016). Assessment of global mercury deposition through litterfall. *Environmental Science & Technology*, 50, 8548–8557. <https://doi.org/10.1021/acs.est.5b06351>
- Wang, X., Cawood, P. A., Zhao, H., Zhao, L., Grasby, S. E., Chen, Z. Q., Wignall, P. B., et al. (2018). Mercury anomalies across the end Permian mass extinction in South China from shallow and deep water depositional environments. *Earth and Planetary Science Letters*, 496, 159–167. <https://doi.org/10.1016/j.epsl.2018.05.044>
- Wang, X. D., Cawood, P. A., Zhao, H., Zhao, L. S., Grasby, S. E., Chen, Z. Q., & Zhang, L. (2019). Global mercury cycle during the end-Permian mass extinction and subsequent Early Triassic recovery. *Earth and Planetary Science Letters*, 513, 144–155. <https://doi.org/10.1016/j.epsl.2019.02.026>
- Wignall, P. (2001). Large igneous provinces and mass extinctions. *Earth Science Reviews*, 53, 1–33. [https://doi.org/10.1016/S0012-8252\(00\)00037-4](https://doi.org/10.1016/S0012-8252(00)00037-4)
- Wignall, P. (2005). The link between Large Igneous Province eruptions and mass extinctions. *Elements*, 1, 293–297. <https://doi.org/10.2113/gselements.1.5.293>
- Xu, W., Mac Niocaill, C., Ruhl, M., Jenkyns, H. C., Riding, J. B., & Hesselbo, S. P. (2018). Magnetostratigraphy of the Toarcian stage (Lower Jurassic) of the Llanbedr (Mochras Farm) Borehole, Wales: Basis for a global standard and implications for volcanic forcing of palaeoenvironmental change. *Journal of the Geological Society*. <https://doi.org/10.1144/jgs2017-120>
- Zaferani, S., Pérez-Rodríguez, M., & Biester, H. (2018). Diatom ooze: A large marine mercury sink. *Science*, 361, 797–800. <https://doi.org/10.1126/science.aat2735>
- Zambardi, T., Sonke, J. E., Toutain, J. P., Sortino, F., & Shinohara, H. (2009). Mercury emissions and stable isotopic compositions at Vulcano Island (Italy). *Earth and Planetary Science Letters*, 277, 236–243. <https://doi.org/10.1016/j.epsl.2008.10.023>
- Zheng, W., Gilleaudeau, G. J., Kah, L. C., & Anbar, A. D. (2018). Mercury isotope signatures record photic zone euxinia in the Mesoproterozoic ocean. *Proceedings of the National Academy of Sciences*, 115, 10594–10599. <https://doi.org/10.1073/pnas.1721733115>